ACS APPLIED MATERIALS & INTERFACES

Research Article

www.acsami.org

Effect of Surface Fluorination of TiO_2 Particles on Photocatalitytic Activity of a Hybrid Multilayer Coating Obtained by Sol-Gel Method

Yunfeng Zhu,[†,‡] Filomena Piscitelli,[‡] Giovanna G. Buonocore,[‡,*] Marino Lavorgna,[‡] Eugenio Amendola,[‡] and Luigi Ambrosio[‡]

[†]School of Textile and Materials Engineering, Dalian Polytechnic University, 116034 Dalian, China

[‡]Institute of Composite and Biomedical Materials, National Research Council, P.le E.Fermi 1, 80055 Portici, Naples, Italy

ABSTRACT: A multilayer photoactive coating containing surface fluorinated TiO_2 nanoparticles and hybrid matrices by sol gel approach based on renewable chitosan was applied on poly(lactic acid) (PLA) film by a step wise spin-coating method. The upper photoactive layer contains nano-sized functionalized TiO_2 particles dispersed in a siloxane based matrix. For the purpose of improving TiO_2 dispersion at the air interface coating surface, TiO_2 nanoparticles were modified by silane coupling agent 1H,1H,2H,2H-perfluorooctyltriethoxysilane (FTS) with fluoro-organic side chains. An additional hybrid material consisting of chitosan (CS) cross-linked with 3-glycidyloxypropyl trimethoxy silane (GOTMS) was applied as interlayer between the PLA substrate and the upper photoactive coating to increase the adhesion and reciprocal affinity. The multilayer TiO_2/CS-GOTMS coatings on PLA films showed a thickness of ~4−6 μm and resulted highly transparent. Their structure was exhaustively characterized by SEM, optical microscope, UV−vis spectroscopy and contact angle measurements. The photocatalytic activity of the multilayer coatings were investigated using methyl orange (MeO) as a target pollutant; the results showed that PLA films coated with surface fluorinated particles exhibit higher activity than films with neat particles, because of a better dispersion of TiO_2 particles. The mechanical properties of PLA and films coated with fluorinated particles, irradiated by UV light were also investigated; the results showed that the degradation of PLA substrate was markedly suppressed because of the UV adsorptive action of the multilayer coating.

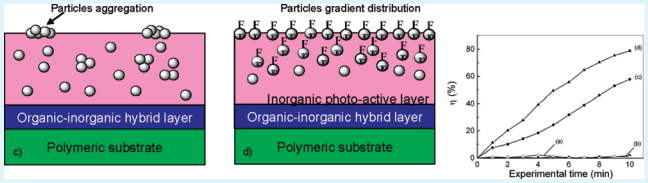

KEYWORDS: *photocatalysis, TiO_2 nanoparticles, surface fluorination, multilayer coating*

1. INTRODUCTION

Because of its high photocatalytic activity, the fascinating inorganic semiconductor titanium dioxide (TiO_2) has been widely used for mineralization of organic compounds in solution.[1] The use of TiO_2 photocatalyst in the form of powder leads to the difficulty of withdrawing the catalyst at the end of the photocatalytic reaction.[2] Therefore, the preparation of supported TiO_2 films is necessary in order to expand its application fields. Nowadays, the TiO_2 is widely used as supported photocatalyst onto inorganic and metallic substrates such as glass, activated carbon fiber, stainless steel, clay, alumina, silicon wafer, and zeolite.[3−9] In recent years, because of the increasing application and development of coating technology, immobilization of TiO_2 particles or deposition of TiO_2 photoactive film also on plastic substrates has become possible. Langlet et al.[10] prepared transparent photocatalytic films deposited on polycarbonate (PC) from sol-gel processed titania sols. Chun et al.[11] deposited TiO_2 thin films on polyethylene terephthalate (PET) and polymethylmetacrylate (PMMA) substrates by nanoparticle deposition system (NPDS). Yu et al.[12] fixed preformed nanocrystalline TiO_2 on low density polyethylene (LDPE) film by heating the LDPE film up to the flowing point in an isopropanol containing TiO_2. The key challenges that have to be faced during the design of photocatalytic coatings for polymeric substrates include two different aspects: (i) it is mandatory to protect the polymeric substrates from photocatalytic oxidative degradation,[13] (ii) it is important to obtain acceptable reaction kinetics during photocatalysis, because, generally, the activity of immobilized TiO_2 particles is lower than that of suspensions.[14] Many approaches have been proposed to solve the above problems. These include both the use of inert polymers that are resistant to the photocatalytic oxidative degradation and the introduction of intermediate protective layers between the TiO_2 active coating and substrate. Paschoalino et al.[15] incorporated TiO_2 (P-25 from Degussa) into polydimethylsiloxane (PDMS) and orthophthalic polyester (OP) polymers and then the film was deposited by spin coating. The obtained films showed high photocatalytic activity in degrading both aqueous phase pollutants (containing dichloroacetic acid, salicylic acid and phenol) and gaseous phase ethanol vapor as well as a high resistance to UV degradation. Iketani et al.[16] prepared TiO_2/PDMS hybrid films on PMMA substrate. These materials showed good photocatalytic activity for decomposition of methylene blue and acetaldehyde, whereas photodegradation of PMMA substrate was greatly suppressed by the hybridization. Yu et al.[17,18] selected Tedlar, consisting of polyvinyl-fluoride units $(-CH_2-CHF-)_n$, and Parylene-C, having as repetitive

Received: September 3, 2011
Accepted: November 25, 2011
Published: November 25, 2011

units, 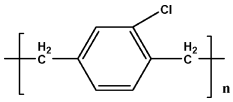 as polymeric substrate to prepare composite photocatalysts. The resulting films are shown to be useful in decolorization of azo dyes. Sánchez et al.[13] deposited photoactive layer of TiO_2 on PET monoliths, by using a protective layer of SiO_2 to prevent oxidation of the substrate.

A big challenge in the development of photocatalytic materials based on TiO_2 particles is the need to enhance their photocatalytic activity, which is strictly related to the exposed surface of titania particles at the coating/air interface. A possible approach to reach this goal is the surface fluorination of TiO_2 particles; in the literature, in fact, it has already been reported the tendency of fluorine containing groups to migrate onto the film/air interface. Toselli et al.[19] demonstrated that the fluorinated segments of poly(caprolactone-b-perfluoropolyether-b-caprolactone) (PCL-PFPE-PCL) triblock copolymers tend to migrate to the outer surface due to the strong thermodynamic driving force to minimize the surface energy. Moreover, Fabbri et al.[20] prepared a perfluoropolyether-based organic-inorganic hybrid by sol−gel process. Their results showed a strong surface segregation of perfluoropolyether (PFPE) because of a marked thermodynamic incompatibility of fluorinated polymer with most of common organic polymers and solvents other than with water and aqueous solution. This leads to the obtainment of a fluorine-rich surface that exhibits enhanced hydrophobicity and lipophobicity. The surface segregation of PFPE segments depends on the chain mobility and on the viscosity of the medium and therefore on the time of reaction before coating application, as well as on solvent evaporation. The use of fluorine containing groups for the preparation of ceramers by sol-gel method has been reported by Whjcik and Klein[21] who prepared water repellent organic-inorganic hybrids based on PFPE diol diacrylate and on perfluoroalkylsilane. Mascia and Tang[22] also studied a cross-linked epoxy resins-silica hybrids obtained with the addition of small amounts of a silane functionalized perfluoroether oligomer. They found an extensive migration of perfluoroethers additive to the surface prior gelation of the silica phase. Schmidt et al.[23] presented a technique for the preparation of photocatalytic gradient coatings based on small particles of titania whose surface has been fluorinated. They prepared transparent coating systems applicable on PC surface by a spray technique. After application of the coating sol, the different solvents evaporate with different rates from the wet film. This results in a gradual change in the balance between polar and nonpolar compounds, finally leading to a thermodynamically driven decompatibilisation of the fluoride functional particles with respect to the matrix. Thus the formation of a self-organizing gradient layer in which photoactive particles enriched on the interface between air and coating is achieved, whereas an inorganic barrier layer was formed between photoactive layer and substrate.

The above mentioned studies dealt with the use of synthetic polymer substrates to support TiO_2 for photocatalytic application, whereas in the literature, only a few papers deal with the use of biomaterials.[24] The growing attention paid to the ecological impact of polymer materials and the recent explosion in prices of petroleum products provoked a strong interest in the field of green materials and biopolymers. For this reason, in this study, a new photoactive multilayer coating has been designed by exploiting potentiality to use both poly(lactic acid) (PLA) obtained from renewable sources[25] as substrate and the biopolymer chitosan[26] as component of an intermediate layer. In detail, a cross-linked chitosan-siloxane hybrid obtained by sol-gel method was coated on PLA as intermediate layer using spin-coating technique. The surface of TiO_2 nanoparticles was functionalized with 1H,1H,2H,2H-perfluorooctyltriethoxysilane. Then the functionalized particles were dispersed in siloxane sol obtained by prehydrolyzing tetraethoxysilane (TEOS) and 3-glycidyloxypropyl trimethoxy silane (GOTMS) and deposited onto the intermediate layer using spin-coating technique. During the evaporation of the solvents, the surface fluorinated TiO_2 particles segregate at the interface between the upper coating and air, finally leading to a TiO_2 enriched surface thus exhibiting high photocatalytic activity. The photoactive multilayer coating characterized by the TiO_2 gradient distribution profile and a better dispersion of nanoparticles at the air-coating interface, is represented in Scheme 1 in comparison with the case wherein the TiO_2 nanoparticles are not functionalized. The structure, the photocatalytic activity, and the stability of the photoactive multilayer coatings were comprehensively evaluated through several analytical and instrumental approaches.

Scheme 1. Schematic Representation of the Multilayer Functional Coating: (a) TiO_2 Particles without Surface Functionalization, (b) Surface-Fluorinated TiO_2 Particles

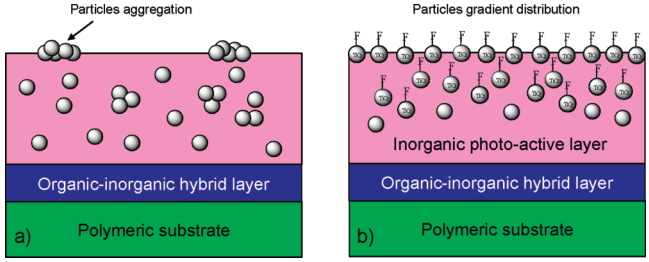

2. EXPERIMENTAL SECTION

2.1. Materials. (a) Titanium dioxide (Degussa P90), mostly in the anatase form, with a specific surface area (BET) of 90 ± 20 $m^2\ g^{-1}$, corresponding to an average primary particle size of ca. 14 nm, was purchased from Evonik Degussa GmbH; (b) Chitosan (CS, medium molecular weight, deacetylation of 75-85%), 3-glycidyloxypropyl trimethoxy silane (GOTMS, 98%), glacial acetic acid, tetraethoxysilan (TEOS, 98%), ethanol (absolute), hydrochloric acid (37%), 1H,1H,2H,2H-perfluorooctyltriethoxysilane (FTS, 98%), dibutyltin dilaurate (DBTDL), anhydrous toluene (99.8%), 2-butanon (99%), and methyl orange (MeO) were purchased from Sigma-Aldrich (Italy) and c) NatureWorks Poly(L-lactide) polymer 2002D was supplied by Cargill Dow LLC (Minnetonka, MN). All products were used as received.

2.2. Surface Fluorination of TiO_2 Particles. A certain amount of P90 TiO_2 particles (dried at 120 °C for 2 h before use) were dispersed in anhydrous toluene under ultrasonic vibrations (MISONIX ultrasonic liquid processors, USA.) at room temperature for 10 min. The TiO_2 slurry was then diverted into a single-necked, round-bottom flask equipped with a magnetic Teflon-coated stirrer. 30 wt % of FTS coupling agent (based on the content of TiO_2) was added. Stirring treatment with a rate of 300 rpm continued for 4 h at 60 °C. Subsequently, the TiO_2 slurry was filtered, dried and then purified by Soxhlet extraction with ethanol for 1 week to remove the FTS physically absorbed on the particles surface. The surface fluorinated TiO_2 particles, which were named as F−P90, were finally obtained by removing the solvent under vacuum in an oven at 50 °C overnight.

2.3. Preparation of Multilayer Coatings. *2.3.1. Preparation of Chitosan-Siloxane Hybrids (CS-GOTMS) for the Intermediate Coating.* Chitosan was dissolved in an acetic acid aqueous solution (1% v/v) to form a chitosan solution of 2 wt %. The prehydrolysis

solution of GOTMS was prepared by mixing 3.198 g of H_2O, 3.1074 g of ethanol and 7 g of GOTMS. The pH of the mixture was adjusted to 4 by the addition of dilute HCl while constant stirring. The mixture was stirred at 500 rpm and 60 °C for 4h and then cooled to room temperature. Subsequently, colloidal dispersion was mixed with the chitosan solution and stirred at 500 rpm and 80 °C for 4 h. CS-GOTMS hybrid sols with various contents of GOTMS (20, 40, 60, and 80 wt %) were synthesized. After cooling, the mixture was ready to be used. However, for specific characterization, it was poured onto glass discs and dried at room temperature for 24 h and then at 50 °C for another 24 h under vacuum until a self-standing film was obtained.

2.3.2. Deposition of the Intermediate Coating on PLA Films. The PLA membranes (thickness of 200−300 μm) were prepared by compression molding using a Collin P300P press at 180 °C and at 40 bar for 3 min, cooled down for 10 min at 10 °C min^{-1} and 10 bar. Circular PLA membranes (diameter of 5 cm, weight of 500 mg) were thoroughly washed with deionized water and ethanol and then dried under ambient conditions before the hybrid coatings were deposited. After selection of the CS-GOTMS hybrid containing 80 wt % of GOTMS (please see Results and Discussion section), the hybrid sols were diluted by adding ethanol (30 wt % on the total weight of chitosan and GOTMS mixture) and then applied onto PLA membranes using a spin coater (CEE Cost Effective Equipment 100, USA, 2000 rpm, 25 r s^{-1}, 90 s). The coated PLA membranes were dried first at room temperature for 2 h and then at 50 °C for 24 h. The final samples were coded as CS-GOTMS/PLA films.

2.3.3. Preparation and Deposition of the Photocatalytic Coating. The precursor solution of the siloxane matrix of the photocatalytic coating was prepared by mixing TEOS, GOTMS, and H_2O at a molar ratio of 1:1.5:8.5. Ethanol was added as cosolvent at double weight of H_2O and DBTDL was added as catalyst. The pH of the mixture was adjusted to 5−6 by the addition of dilute HCl while constant stirring. The mixture was stirred at 500 rpm and 60 °C for 4 h, cooled to room temperature, and then stored for 24 h at ambient conditions.

A certain amount of photocatalysts (P90 and F−P90) were dispersed in 2-butanon under ultrasonic treatment in an ice bath for 10 min to obtain dispersions with concentration of 10, 20, and 40 mg L^{-1}. Subsequently, 5 g of the photocatalysts dispersion was added in 24.5 g of the sols of TEOS and GOTMS, precursors of the siloxane matrix and then subject to ultrasonic irradiation in an ice bath for 10 min to obtain a homogenous dispersion. The application of the photocatalytic coating (1.5 mL of dispersion) on CS-GOTMS/PLA films was carried out by spin coating (1000 rpm, 25 r s^{-1}, 60 s). The multilayer coated PLA films were dried first at room temperature for 2 h and then at 50 °C for 24 h. The final samples were coded as P90/CS-GOTMS/PLA and F−P90/CS-GOTMS/PLA, respectively, for films containing unfluorinated and surface-fluorinated TiO_2 particles.

2.4. Experimental Characterization. Thermogravimetric analysis (TGA) was performed using a TA Instruments Q500 thermal analysis apparatus. The samples were heated over the temperature range from 40 to 750 °C at a rate of 10 °C min^{-1} in a nitrogen atmosphere.

Fourier transform infrared (FTIR) spectra of the purified P90 and FP90 powders were collected with a Nicolet FTIR spectrometer in the range from 4000 to 400 cm^{-1}. The KBr pellets were prepared using dried samples (≅1 wt %).

XPS measurements were carried by using an ESCALAB MKII (VG Scientific Ltd, UK) spectrometer with Al Kα excitation source and a 5-Channeltron detection system. Photoelectron spectra were collected at 20 eV constant pass energy of the analyzer. The spectra were processed by the CasaXPS software by using a peak fitting routine with symmetrical Gauss-Lorentian function.

Contact angle measurements were carried out by using a DataPhysics OCA 20 apparatus. Distilled water was dropped onto at least 5 different sites on each sample, and the static contact angle was reported as the average value from the measured values.

The water liquid uptake was calculated from eq 1:

$$\text{water uptake} = \frac{W_w - W_d}{W_d} \cdot 100 \quad (1)$$

where W_w and W_d are the weight of the wet and dry films, respectively. The weight of the dry film was determined by weighting the samples after desiccation overnight under vacuum. The dried membranes were then saturated in water at 30°C for 24 h. Then the membrane was taken out of the water, wiped quickly with filter paper and weighted to determine the wet weight. The data reported were the mean values of three replicates.

The UV−vis spectra of the films were recorded in transmittance mode by a PerkinElmer Lambda 900 UV−vis spectrometer.

A field emission scanning electron microscope (FESEM) was used to characterize the morphology of the multilayer photocatalytic coating. The PLA coated films were immersed in liquid nitrogen and fractured for the SEM observation (FEI QUANTA 200F).

A self-regulating UV irradiation instrument was used to investigate the stability of the coating. In particular, the samples were exposed to eight 15 W UV lamps (Actinic BL, Philips) emitting long-wave UV-A radiation in the 350-400 nm range which were installed at 20 cm away from the samples.[28] The temperature at sample surface was monitored and it was found to be approximately 50°C. After UV irradiation, tensile testing of film samples was carried out by using an electro-mechanical universal testing machine SANS CMT4304 (Shenzhen SANS Testing Machine Co. Ltd., China) at room temperature according to ASTM Standard D1708-06a. The separation speed of the two grips was maintained at 1.3 mm min^{-1} for each test, and the data reported were the mean values of ten determinations.

2.5. Photocatalytic Activity. An aqueous solution of MeO was used as a model contaminant for studying photocatalytic activities of the multilayer coatings deposited on the PLA films. Photocatalysis experiments were carried out by using self-regulating UV irradiation instrument previously described. A quartz pan containing both 10 mL of a 5 ppm MeO solution and the film (5 cm diameter) was placed under the UV lamps. The intensity of the radiation reaching the solution surface was 3.4 mW cm^{-2} and was detected by a GOLDILUX GPR-1 radiometer equipped with a UV-A probe. The change in the concentration of MeO was monitored by measuring the absorbance at λ_{max} = 464 nm with a SCINCO S-3100 UV−vis spectrophotometer. The extent of MeO degradation or decolorization degree was calculated by using the following equation

$$\eta = \frac{A_0 - A_t}{A_0} \cdot 100 \quad (2)$$

where A_t is the absorbance of the MeO solution at reaction time t, and A_0 is the absorbance of the initial 5 ppm MeO solution.

3. RESULTS AND DISCUSSION

3.1. Characterization of the Surface-Fluorinated TiO_2 Nanoparticles. As described in Scheme 1, the TiO_2 particles were modified by silane coupling agent FTS in order to decrease their polarity and to delay their sedimentation rate, thus allowing the formation of a coating with a TiO_2 gradient profile distribution and a better particle distribution at the upper side.[23] The FTS molecule has ethoxy groups which can react with hydroxyl groups present on the surface of TiO_2 particles through several reaction mechanisms (Scheme 2 reports a simplified representation of TiO_2 surface modification by FTS). Neat and surface fluorinated TiO_2 particles (P90 and F−P90) were analyzed by TGA, FTIR, and XPS.

Figure 1 shows the TGA curves of P90 and F−P90 nanoparticles. The P90 sample (Fig. 1a) shows a total weight loss of ∼3.4 wt %, which may be attributed to the removal of physically adsorbed water and the condensation of OH groups present on the surface of the sample. As for the F−P90 particles (Figure 1b), the weight loss between 50 and 200 °C is attributed to the water evaporation, whereas the weight loss of ∼9 wt % in the range of 200−750 °C is attributed to the thermal decomposition of grafted FTS organic moieties as well

Scheme 2. Schematic Representation of Surface Modification of TiO_2 by FTS

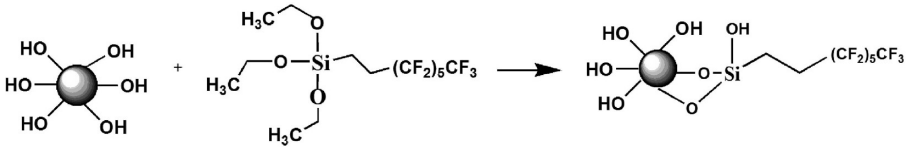

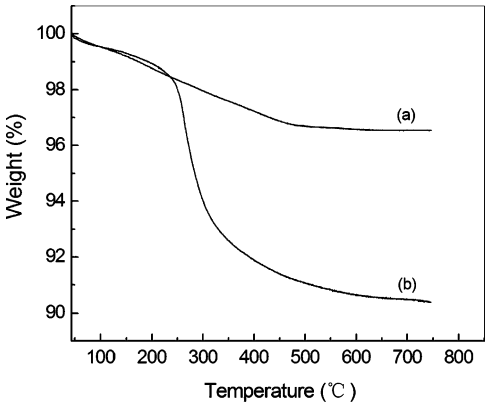

Figure 1. Thermogravimetric analysis curves of (a) P90 and (b) F−P90.

as the condensation of residual OH groups still present on the surface of TiO_2 particles. The content of organic moieties due to the fluorination of TiO_2 particles can be estimated in the range between 9 wt % (if all OH groups present on TiO_2 surface react with FTS silane) and 7 wt % (if all OH groups are unreacted and FTS molecules are only physically absorbed on the surface of TiO_2 particles).[27]

Figure 2 illustrates the FT-IR spectra of (a) P90 and (b) F−P90 nanoparticles. The bands which confirm the presence of

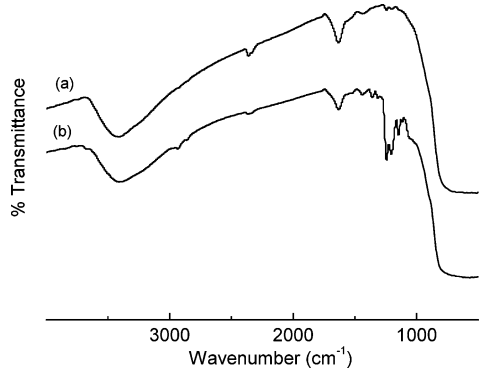

Figure 2. FTIR spectra of (a) P90 and (b) F−P90.

FTS in the F−P90 nanoparticles are centered at ca. 2840−2930 cm^{-1}, 1200−1350 cm^{-1}, and 1080−1200 cm^{-1} and are assigned to the C−H stretching mode, $-CF_2-$, and $-CF_3$ asymmetric stretching mode and symmetric stretching mode, respectively. The spectra of F−P90 nanoparticles also show the characteristic broad absorption bands of Ti−O−Ti at around 400−500 cm^{-1} and −OH groups at 3000−3500 cm^{-1}.[29]

The surface composition of P90 and F−P90 nanoparticles was determined by XPS and the percentage atomic amounts of Ti, O, F on the surface of P90 and F−P90 nanoparticles are reported in Table 1. It is shown that only Ti and O elements were detected on the surface of P90 particles, while the F

Table 1. Surface Composition of P90 and F−P90 Composites[a]

element	percentage (%)	
	P90	F−P90
Ti	27.1	18.6
O[b](oxide)	46.1	43.2
O[b] (water and OH groups)	26.8	5.3
F	not detected	32.9

[a]Si content is not detected for sample F−P90, as it is lower than the detection limit. [b]The O content refers to the total O1s at 530.3 eV (oxide) and 532.6 eV (water and OH groups).

element was detected in the case of F−P90 nanoparticles. Additionally, the percentage atomic amounts of Ti and O elements on the surface of the F−P90 nanoparticles decreases in comparison to P90 particles because of the coverage of the TiO_2 surface particles due to FTS moieties; in particular a significant reduction of OH can be observed groups in the case of F−P90 nanoparticles because of the fluorination reaction.

3.2. Characterization of CS-GOTMS Hybrid. The mechanism involved in the preparation of CS-GOTMS hybrid has been detailed in the previous literature.[30,31] Under acidic condition, the GOTMS hydrolyses to form silanol groups and, after mixing with chitosan solution, the oxirane rings of GOTMS react with chitosan amino groups. Afterwards, thermal treatments allow the silanol groups to form Si−O−Si covalent bonds, and finally, the material results in a organic-inorganic cross-linked structure.

In this study, CS-GOTMS hybrid was prepared as matrix for the intermediate layer deposited in between the PLA substrate and photocatalytic coating. Hence, this layer must exhibit the following peculiar characteristics: (a) a reduced water liquid uptake to allow its use under water exposure; (b) an optimized hydrophilicity to improve the compatibility with the photocatalytic coating. For these reasons, the water liquid uptake and water contact angle of CS-GOTMS hybrid were investigated and the results are shown in Figure 3. Chitosan films absorb large amounts of water and ultimately dissolves in water after 24 h; conversely, the CS-GOTMS hybrid structure induces a significant depression of the swelling capability of chitosan. In particular, the water uptake of the hybrid decreases linearly with increasing the GOTMS content (i.e., the water uptake decreases of 20 wt % as the GOTMS content in the hybrid increases of 20 wt %). Moreover, the contact angle of water on the surface of CS-GOTMS hybrid samples also decrease with an increase in GOTMS content. A water liquid uptake of 22.3% and a contact angle of 59.7°, which are significantly lower than the water uptake of pure CS and contact angle of PLA (75.1°), respectively, were achieved when the mass percentage of GOTMS based on CS was 80 wt %.

The thermal stability of CS-GOTMS hybrids was assessed by TGA in nitrogen atmosphere, and the results are reported in Figure 4. The weight loss in the temperature range 40-150 °C and 150-700°C are associated with the evaporation of adsorbed

dx.doi.org/10.1021/am201192e | ACS Appl. Mater. Interfaces 2012, 4, 150−157

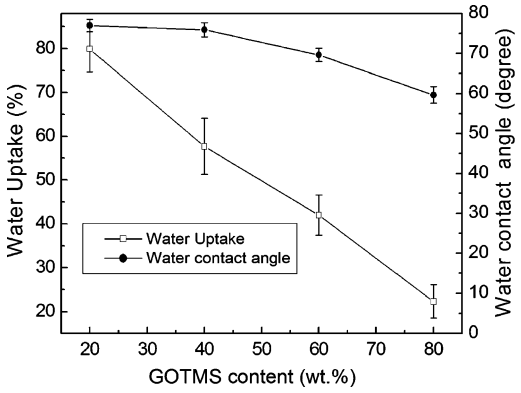

Figure 3. Plots of water contact angle and water uptake as a function of GOTMS contents for CS-GOTMS hybrid.

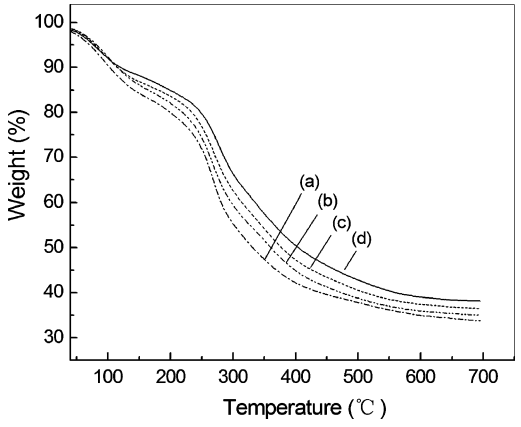

Figure 4. Thermogravimetric analysis curves of CS-GOTMS hybrid with different GOTMS contents: (a) 20, (b) 40, (c) 60, and (d) 80%.

Table 2. Char Yards and Decomposition Temperature at 20 and 50% Weight Loss of CS-GOTMS Hybrid with Different Contents of GOTMS

GOTMS content (%)	temperature at 20% weight loss (°C)	temperature at 50% weight loss (°C)	char yard at 695 °C (%)
20	199	333	33.7
40	217	361	35
60	233	379	36.5
80	248	408	38.1

water and the degradation of chitosan backbone respectively. The temperature at 20 and 50% weight loss and the char yield at 695 °C (reported in Table 2) increase with an increase in GOTMS content. The formation of high degree of inorganic crosslinked structures results in the improvement of the hybrid thermal stability. The increase of the char yield with the GOTMS content is attributed to the presence of siloxane domains dispersed in the chitosan matrix which are thermally converted in stable silica.[30] The TGA results confirm that the organic and inorganic phase are intimately connected and cooperate sinergically to enhance the properties of the obtained CS-GOTMS hybrid.

3.3. Characterization of the Multilayer TiO_2/CS-GOTMS Coating on PLA Films. Figure 5 and Figure 6 show respectively a representative cross-section SEM and optical graphs of TiO_2/CS-GOTMS coated PLA films. Figure 5 shows that the surface of PLA substrate is covered by a coating layer with a total thickness of ~4−6 μm. Figure 6 shows an

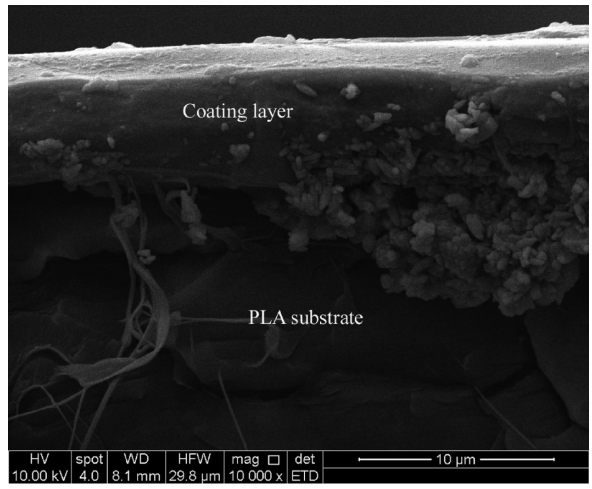

Figure 5. Typical SEM micrograph for the cross-section of TiO_2/CS-GOTMS-coated PLA membrane.

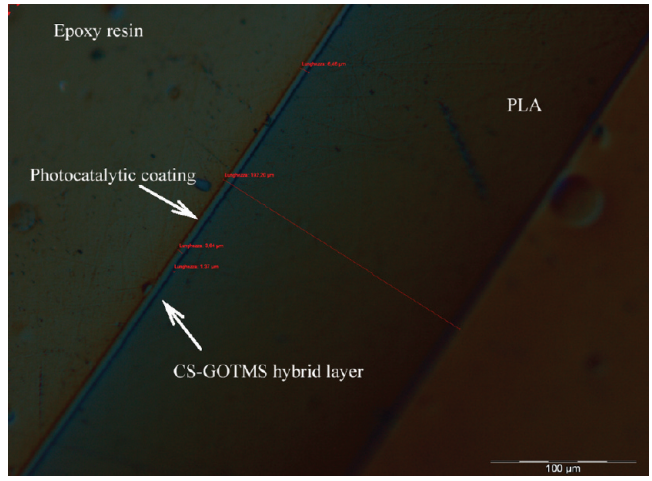

Figure 6. Typical optical micrograph for the cross-section of TiO_2/CS-GOTMS-coated PLA membrane.

evident three layers structure, consisting of a PLA substrate with a thickness of ~180 μm, a CS-GOTMS intermediate layer with a thickness of ~1−2 μm, and a photocatalytic coating with a thickness of ~3−4 μm. Moreover, the total thickness of two coating layers is consistent with the thickness observed in SEM graph.

The surface morphology of P90/CS-GOTMS/PLA and F−P90/CS-GOTMS/PLA films was also observed by SEM, as shown in Figure 7. In both cases, the surface morphologies are undamaged, without any cracks. Additionally, significant particle agglomerates are observed on the surface of P90/CS-GOTMS/PLA membrane, indicating that only poor dispersion of P90 nanoparticles was obtained during the coating preparation. Conversely, in the case of F−P90/CS-GOTMS/PLA films, F−P90 nanoparticles were homogeneously dispersed throughout the sample surface.

The UV−vis transmittance spectra of the PLA, CS-GOTMS/PLA films and F−P90/CS-GOTMS/PLA films containing different amounts of F−P90 particles are displayed in Figure 8. Pure PLA shows high transmittance at the wavelength higher than 250 nm, indicating that nearly all the UV−B (280−315 nm), UV-A (315−400 nm), and visible light passes through the film thickness. The CS-GOTMS intermediate coating layer

dx.doi.org/10.1021/am201192e | ACS Appl. Mater. Interfaces 2012, 4, 150−157

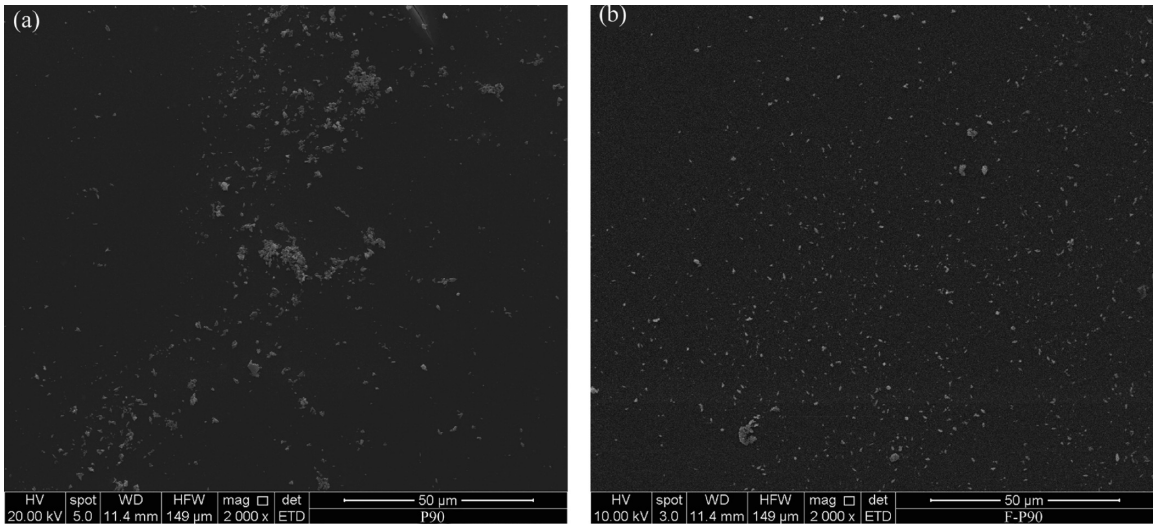

Figure 7. SEM micrographs for the surface: (a) P90/CS-GOTMS/PLA and (b) F−P90/CS-GOTMS/PLA membranes.

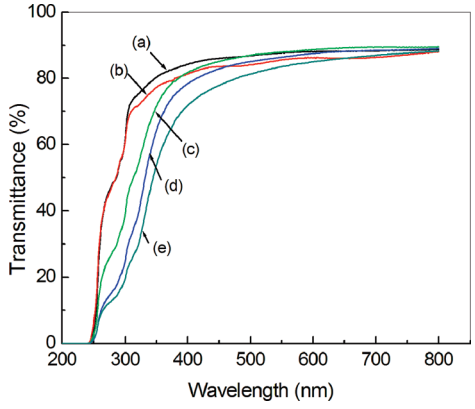

Figure 8. UV−vis transmittance spectra of (a) PLA, (b) CS-GOTMS/PLA films, and F−P90/CS-GOTMS/PLA with different concentrations of F−P90: (c) 10, (d) 20, and (e) 40 mg/L.

reduces only slightly the transmittance of PLA at the wavelength higher than 300 nm. This is due to the presence of the cross-linked hybrid structure and the possible reflection and scattering effects due to some larger siloxane domains. The presence of the upper photocatalytic TiO_2 coating modifies the spectrum profile of PLA; F−P90/CS-GOTMS/PLA films show a significant decrease of the transmittance in UV region, which is attributed to the characteristic absorption of TiO_2 band gap (anatase, 3.2 eV) at ca. 380 nm. The larger the amount of F−P90 particles, the higher the transmittance decreases in the UV. It is worth noting that the multilayer coatings are highly transparent in the visible light region and do not affect the original transparency of the substrate. This is a very important feature for the real application of the multilayer photoactive coating.

The hydrophilicity of the photoactive surface of the multilayer coatings was examined by measuring the contact angle, as shown in Figure 9. The water contact angle of P90/CS-GOTMS/PLA and F−P90/CS-GOTMS/PLA film was respectively 65.1 and 97.1°, indicating that the presence of F−P90 homogeneously dispersed make the multilayer coating surface highly hydrophobic. This result confirms that after the application of upper photocatalytic coating containing F−P90 particles, because of evaporation of solvents, a thermodynamically driven decompatibilisation of the fluoride functional particles with respect to the matrix takes place and leads to an homogenous distribution of fluorinated photoactive particles at the interface between air and coating.[23]

3.4. Photocatalytic Activity of the Multilayer Coating on PLA Film. In this study, the photocatalytic activitiy of TiO_2/CS-GOTMS-coated PLA films were evaluated by the degradation of MeO under UV irradiation. Before starting the tests, some control experiments in which the MeO solution was kept under UV illumination without any photocatalytic film were performed. The results show that no appreciable degradation of MeO was observed after 10 h. Thus, the MeO dye can be considered stable to photolysis. As further experiment control, the degradation of MeO under dark exposure was also assessed.

Figure 10 shows the decolorization degree of MeO (η) as function of the exposure time at the darkness as well as of the UV-irradiation time. No significant decolorization of MeO was observed in the presence of P90/CS-COTMS/PLA or F−P90/CS-COTMS/PLA films exposed at the darkness (curves a and b), indicating that the adsorption of MeO by the two films is negligible. Conversely a continuous increase of decolorization of MeO was observed for P90/CS-COTMS/PLA or F−P90/CS-COTMS/PLA films under UV light irradiation

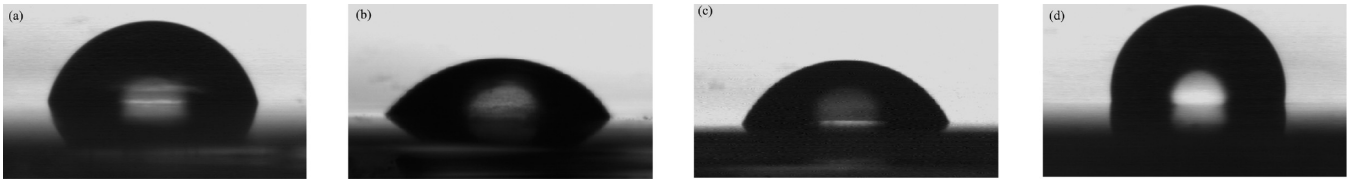

Figure 9. Contact angles of (a) PLA (75.1°), (b) CS-GOTMS/PLA (59.7°), (c) P90/CS-GOTMS/PLA (65.1°), and (d) F−P90/CS-GOTMS/PLA (97.1°) films.

dx.doi.org/10.1021/am201192e | ACS Appl. Mater. Interfaces 2012, 4, 150−157

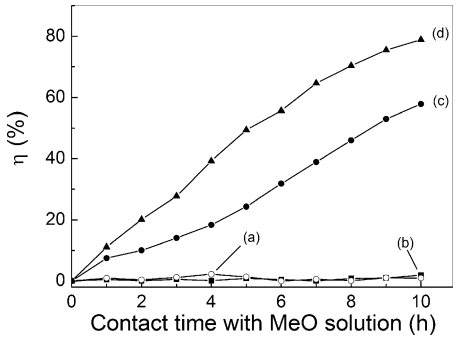

Figure 10. Decolorization degree of MeO vs. contact time between the coated PLA and the MeO solution (initial TiO_2 concentration is 20 mg/L). (a) Dark adsorption in the presence of P90/CS-GOTMS/PLA film; (b) dark adsorption in the presence of F−P90/CS-GOTMS/PLA coating; (c) degradation degree under UV light irradiation in the presence of P90/CS-GOTMS/PLA film; (d) degradation degree under UV light irradiation in the presence of F−P90/CS-GOTMS/PLA film (relative error ± 3%).

(curve c and d). After 10 h of UV-irradiation, the decolorization degrees of MeO for P90/CS-COTMS/PLA and F−P90/CS-COTMS/PLA films were 58 and 79%, respectively. This indicates that the hybrid multilayer coatings are active and able to degrade MeO under UV irradiation. Moreover, F−P90/CS-COTMS/PLA films exhibit a photoactivity higher than P90/CS-COTMS/PLA films due to the better surface distribution of TiO_2 particles determined by the fluorination of TiO_2 surface. As discussed above, during the drying of the wet films, the F−P90 particles move to the interface between the coating and air and gather homogeneously at the surface of the multilayer coating. Thus, the photo-generated reactive radicals are easy to come in contact and react with MeO within their lifetime and this results in the higher activity of the films.

Figure 11 shows the decolorization of MeO as a function of UV-irradiation time for F−P90/CS-COTMS/PLA films with

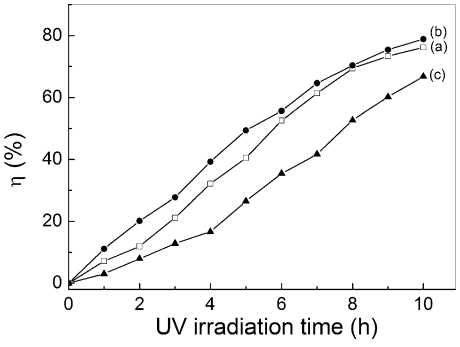

Figure 11. Effect of TiO_2 loading on the decolorization degree of MeO under UV light irradiation in the presence of F−P90/CS-COTMS/PLA films: (a) 10, (b) 20, and (c) 40 mg/L (relative error ± 3%).

different amounts of F−P90 particles. After 10 h of UV-irradiation, the decolorization rate shows a maximum with the F−P90 amount. In particular, the decolorization degrees of MeO for F−P90/CS-COTMS/PLA films were 76, 79, and 67%, respectively, for the samples containing of 10, 20, and 40 mg/L of F−P90 particles. The increase in the F−P90 concentration from 10 to 20 mg/L favors the photocatalytic degradation of MeO. This is attributed to the increase in the number of effective active particles which participate in the photocatalytic reaction. When the concentration of F−P90 is higher than 20 mg/L, the observed decrease in the photocatalytic activity may be attributed to the probable occurring of particles aggregation on the surface of coating.

Photodegradation results can be compared with those obtained by Zhu et al.[28] who developed active films embedding TiO_2 particles into PLA films by compression molding and extrusion techniques. The authors showed that after 10 h of UV-irradiation, only the film loaded with 10 wt % of TiO_2 particles was able to reach a decolorization degree of 80%, whereas in the present paper, the same decolorization degree has been achieved by the developed multilayer photoactive films that contain a TiO_2 percentage of approximately 0.002 wt %. This result proves a great enhancement of the photocatalytic activity, thus confirming the validity of the proposed approach.

The effectiveness of photocatalytic activity of F−P90/CS-GOTMS/PLA films exposed to 10 h cycles of UV irradiation was investigated and the results are shown in Figure 12. The

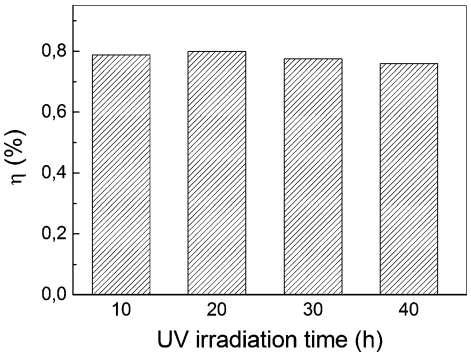

Figure 12. Repetitive decolorization of MeO under UV light irradiation in the presence of F−P90/CS-COTMS/PLA films (initial TiO_2 concentration is 20 mg/L) (relative error ± 3%).

films were washed after each photoaging cycle and then the dye solution was renewed to carry out a successive decolorization cycle. The results indicated that the decolorization degree remained stable after 4 cycles and the photoactivity was not affected by aging for UV exposure.

3.5. Mechanical Properties of Multilayer Coated PLA Films Aged under UV Irradiation. The mechanical properties of PLA and F−P90/CS-COTMS/PLA films UV-aged were evaluated as function of the UV-irradiation time. The average values of the tensile strength and elongation at break are shown in Figure 13. Before UV-irradiation, the coated PLA samples show a reduction of tensile strength compared to the neat PLA. This is ascribed to the imbrittlement of the surface due to the effect of solvents adopted to formulate the intermediate layer[32] and to the effect of the different thermal treatments. After 30 days of UV-irradiation aging, the tensile strength and the elongation at break of PLA films decrease respectively of about 37 and 54%. As for the F−P90/CS-COTMS/PLA films, the tensile strength and elongation at break decrease of about 14 and 17%, respectively. This indicates that the F−P90/CS-COTMS/PLA films exhibit better long-term stability compared with PLA films. The photocatalytic coating absorbs most of UV light, shielding the PLA substrate and improving the UV-aging resistance of F−P90/CS-GOTMS/PLA films. Moreover, the presence of an inorganic layer between the photocatalytic

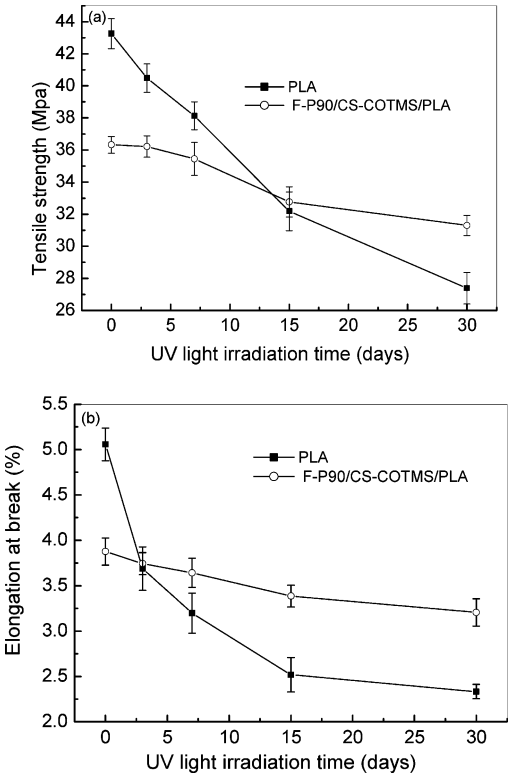

Figure 13. Mechanical properties of PLA and F−P90/CS-GOTMS/PLA films after different UV light irradiation time: (a) tensile strength and (b) elongation at break.

particles and the PLA substrate, acting as a barrier, prevents the photogenerated reactive oxidative radicals to reach and deteriorate the polymer structure.

4. CONCLUSIONS

This study presented a feasible method to deposit a photocatalytic multilayer coating on PLA biodegradable film by using a hybrid biopolymer-based coating in order to increase the adhesion and affinity between the organic PLA substrate and a completely inorganic photoactive coating based on surface fluorinated TiO_2 particles. It has been proven that, because of the better dispersion of the fluorinated TiO_2 particles, F−P90/CS-GOTMS/PLA films exhibits higher activity than that of P90/CS-GOTMS/PLA films. Moreover, it has been shown that TiO_2/CS-GOTMS/PLA films exhibit extremely high transparency in visible light and that the degradation under UV exposure of PLA substrate was markedly suppressed by the deposition of F−P90 photocatalytic coating. The method presented in this study overcomes all drawbacks associated with the use of TiO_2 powder in suspension and the use of embedded TiO_2 particles in polymer matrix and gives rise to materials that can be potentially used for waste water treatment and antibacterial application.

AUTHOR INFORMATION

Corresponding Author

*gbuonoco@unina.it.

REFERENCES

(1) Fujishima, A.; Rao, T. N.; Tryk, D. A. *J. Photochem. Photobiol., C* **2000**, *1*, 1−21.
(2) Yu, Z.; Laub, D.; Bensimon, M.; Kiwi, J. *Inorg. Chim. Acta* **2008**, *361*, 589−594.
(3) Fernández, A.; Lassaletta, G.; Jiménez, V. M.; Justo, A.; González-Elipe, A. R.; Herrmann, J.-M.; Tahiri, H.; Ait-Ichou, Y. *Appl. Catal., B* **1995**, *7*, 49−63.
(4) Zhang, X.; Lei, L. *Appl. Surf. Sci.* **2008**, *254*, 2406−2412.
(5) Anandan, S.; Yoon, M. *J. Photochem. Photobiol., C* **2003**, *4*, 5−18.
(6) Sopyan, I.; Watanabe, M.; Murasawa, S.; Hashimoto, K.; Fujishima, A. *J. Photochem. Photobiol., A* **1996**, *98*, 79−86.
(7) Kato, S.; Hirano, Y.; Iwata, M.; Sano, T.; Takeuchi, K.; Matsuzawa, S. *Appl. Catal., B* **2005**, *57*, 109−115.
(8) Kim, T.-H.; Sohn, B.-H. *Appl. Surf. Sci.* **2002**, *201*, 109−114.
(9) Neela Priya, D.; Modak, J. M.; Raichur, A. M. *ACS Appl. Mater. Interfaces* **2009**, *1*, 2684−2693.
(10) Langlet, M.; Kim, A.; Audier, M.; Guillard, C.; Herrmann, J.M. *Thin Solid Films* **2003**, *429*, 13−21.
(11) Chun, D.M.; Kim, M.H.; Lee, J.C.; Ahn, S.H. *CIRP Ann.−Manuf. Techn.* **2008**, *57*, 551−554.
(12) Yu, Zhiyong; Mielczarski, E.; Mielczarski, J.; Laub, D.; Buffat, P.; Klehm, U.; Albers, P.; Lee, K.; Kulik, A.; Kiwi-Minsker, L.; Renken, A.; Kiwi, J. *Water Res.* **2007**, *41*, 862−874.
(13) Sánchez, B.; Coronado, J.M.; Candal, R.; Portela, R.; Tejedor, I.; Anderson, M.A.; Tompkins, D.; Lee, T. *Appl. Catal., B* **2006**, *66*, 295−301.
(14) Mazille, F.; Schoettl, T.; Pulgarin, C. *Appl. Catal., B* **2009**, *89*, 635−644.
(15) Paschoalino, M.P.; Kiwi, J.; Jardim, W. F. *Appl. Catal., B* **2006**, *68*, 68−73.
(16) Iketani, K.; Sun, R.D.; Toki, M.; Hirota, K.; Yamaguchi, O. *J. Phys. Chem. Solids* **2003**, *64*, 507−513.
(17) Yu, Z.; Mielczarski, E.; Mielczarski, J.A.; Laub, D.; Kiwi-Minsker, L.; Renken, A.; Kiwi, J. *J. Mol. Catal. A: Chem.* **2006**, *260*, 227−234.
(18) Yu, Z.; Keppner, H.; Laub, D.; Mielczarski, E.; Mielczarski, J.; Kiwi-Minsker, L.; Renken, A.; Kiwi, J. *Appl. Catal., B* **2008**, *79*, 63−71.
(19) Toselli, M.; Messori, M.; Bongiovanni, R.; Malucelli, G.; Priola, A.; Pilati, F.; Tonelli, C. *Polymer* **2001**, *42*, 1771−1779.
(20) Fabbri, P.; Messori, M.; Montecchi, M.; Nannarone, S.; Pasquali, L.; Pilati, F.; Tonelli, C.; Toselli, M. *Polymer* **2006**, *47*, 1055−1062.
(21) Wojcik, A.B.; Klein, L.C. *Proc. SPIE−Int. Soc. Opt. Eng.* **1996**, *2611*, 172−177.
(22) Mascia, L.; Tang, T. *J. Sol−Gel Sci. Technol.* **1998**, *13*, 405−408.
(23) Schmidt, H.; Naumann, M.; Müller, T.S.; Akarsu, M. *Thin Solid Films* **2006**, *502*, 132−137.
(24) Qi, K.; Xin, J. H. *ACS Appl. Mater. Interfaces* **2010**, *2*, 3479−3485.
(25) Auras, R.; Harte, B.; Selke, S. *Macromol. Biosci.* **2004**, *4*, 835−864.
(26) Tual, C.; Espuche, E.; Escoubes, M.; Domard, A. *J. Polym. Sci., Part B: Polym. Phys.* **2008**, *38*, 1521−1529.
(27) Erdem, B.; Hunsicker, R.A.; Simmons, G.W.; Sudol, E.D.; Dimonie, V.L.; El-Aasser, M.S. *Langmuir* **2001**, *9*, 2664−2669.
(28) Zhu, Y. F.; Buonocore, G.G.; Lavorgna, M.; Ambrosio, L. *Polym. Compos.* **2011**, *32*, 519−528.
(29) Musić, S.; Gotić, M.; Ivanda, M.; Popović, S.; Turković, A.; Trojko, R.; Sekulić, A.; Furić, K. *Mater. Sci. Eng., B* **1997**, *47*, 33−40.
(30) Liu, Y. L.; Su, Y. H.; Lai, J.Y. *Polymer* **2004**, *45*, 6831−6837.
(31) Liu, Y. L.; Su, Y. H.; Lee, K. R.; Lai, J.Y. *J. Membr. Sci* **2005**, *251*, 233−238.
(32) Iotti, M.; Fabbri, P.; Messori, M.; Pilati, F.; Fava, P. *J. Polym. Environ.* **2009**, *17*, 10−19.